

# Designing Nonwovens to Meet Pore Size Specifications

Glen E. Simmonds<sup>1</sup>, John D. Bomberger<sup>1</sup>, Michael A. Bryner<sup>2</sup>

<sup>1</sup>E.I. Du Pont de Nemours & Co., Experimental Station, Wilmington, Delaware USA

<sup>2</sup>E.I. Du Pont de Nemours & Co., Richmond, Virginia USA

Correspondence to:

Glen E. Simmonds email: [glen.e.simmonds@usa.dupont.com](mailto:glen.e.simmonds@usa.dupont.com)

## ABSTRACT

New nonwovens applications in areas such as filtration require a media designed to particular pore size specifications in the 3 to 20 micron range. The purpose of this work was to develop a basis by which to design and construct a fabric with given pore size specifications. While doing so we have provided a validation for two different mathematical models. We have also found that bicomponent spunbonded islands-in-the-sea nonwoven fabrics can be designed very precisely to achieve target pore diameters and porosity. Mathematical models can be used to develop fabric specifications in the standard manufacturing terms of basis weight and fiber diameter. Measured mean flow pore diameters for the test fabrics showed excellent correlation to targeted mean flow pore diameters for both models. The experimental fit to the Bryner model is the better of the two, but requires specification of fabric thickness in addition to basis weight and fiber diameter to achieve actual mean pore diameters that closely match target values. Experimental validation of the influence of fabric thickness on the mean flow pore diameter at constant basis weight and fiber diameter remains open for further investigation. In addition, achieving complete separation of the island and sea polymers along with unbundling of the island fibers remain areas for improvement.

## INTRODUCTION

One of the first challenges in designing fabrics to meet a target mean pore diameter and overall porosity is to develop fabric specifications in conventional manufacturing terms, for example, basis weight and fiber diameter. To that end, we derive a model relating fiber thickness and porosity to the mean and maximum pore diameters for a nonwoven sheet. This new model is compared to a model by Lifshutz [1] that empirically relates mean flow pore diameter and hydraulic diameter to fiber size and the sheet basis length, the total length of fiber in a unit area of nonwoven material.

It is generally accepted that one of most direct ways to achieve small pores is by using small fibers. Thus, the use of ever decreasing fiber diameters in nonwoven structures is a well-established trend. One method of creating fibers with diameters of 1 to 10 microns is a bicomponent fiber method known as islands in the sea. These bicomponent fibers typically consist of a group of individual “islands” of one polymer surrounded by a “sea” of a second polymer. Each bicomponent fiber ranges from about 1 to 5 denier. The fibers can be processed as continuous filaments or chopped into staple fibers. In either case, the sea polymer is eventually removed by dissolving it with a solvent or by melting, leaving behind the small island fibers. This paper deals with fabrics of continuous filament, spunbonded, bicomponent webs.

Part 1 of this article presents a model developed by M.A. Bryner and compares it to a model developed by N. Lifshutz. The two models presented diverge in terms of the influence of porosity on the mean pore diameter. Part 2 of this article presents the experimental vs. theoretical results for a series of test fabrics.

## PART 1 - DERIVATION OF A MODEL RELATING PORE DIAMETER AND FIBER DIAMETER IN A NONWOVEN SHEET

The analysis presented here generally follows the approach developed in the literature on paper structure and summarized in the book, *Paper: An Engineered Stochastic Structure*, by Deng and Dodson [2]. The principle difference in this analysis is that while the existing statistical descriptions are developed for very low fiber densities or coverages on a deposition plane, practical application requires extension to higher fiber densities or coverages. Throughout the development presented here, reference and comparison will be made to the pioneering results of Kallmes and Corte [3] who developed an extensive statistical description of paper at low fiber coverages.

## MODEL DEVELOPMENT

### Overview

The approach presented here is first to determine the open pore area. Then the total number of pores is determined. From these two, the mean pore area is established. Pores in nonwoven fabrics are polygons with sides formed by the free length of fibers between crossings. The characteristics of the general nature of the polygons are known, so the number and length of sides is used to determine the average wetted perimeter of a pore. The average perimeter and the pore area are used to determine the pore hydraulic radius from which the mean pore size obtained. The stochastic structure results in a pore size distribution for which the maximum size is known in terms of the mean pore size. Hence the maximum pore size is then determined.

The statistical development is inherently a two dimensional treatment. The effect of all fibers is accounted as if they were in the same plane, the plane of projection. The result is that the idealized pore size diminishes monotonically to zero as the number of fibers deposited gets very large. In reality, the fibers form a three dimensional fabric structure. Deep within the real structure, the pore size in any given plane is independent of the total number of fibers in the fabric. A method is presented for adapting the two dimensional statistical results to three dimensional fabrics. The basis for this is the realization that deep within the porous fabric, the pore structure should appear self-similar to a fluid flowing in either direction perpendicular to the plane of fiber deposition.

### Pore Size from Hydraulic Radius

The objective of this analysis is to relate the pore size of a nonwoven sheet to sheet structure, and in particular, to fiber size and void or solids fraction. One approach is through consideration of the hydraulic radius of a pore,  $R_h$ , which is defined as the ratio of pore area to pore wetted perimeter. The radius of a cylindrical pore is just  $4 R_h$ . In this derivation, pore size is obtained as a hydraulic radius and then related to the equivalent cylindrical pore size.

### Area Fraction Covered by Fibers

In a random deposition of fibers on a plane surface of unit area, the probability that any given point is covered by  $n$  fibers is given by the Poisson distribution function [2],

$$P(n) = \frac{e^{-c} c^n}{n!} \quad (1)$$

where  $c$  is the total projected area of fiber per unit area, commonly termed "coverage." The total projected area of fiber per unit area is the product of projected fiber width  $w$ , fiber length  $\ell$ , and the total number of fibers per unit area  $n_f$ .

$$c = w \cdot \ell \cdot n_f \quad (2)$$

$P(n)$  is also the fraction of the unit area covered by  $n$  fibers, so,  $P(0)$  is the fraction of the unit area not covered by fibers, i.e., the open area fraction  $\xi$ ,

$$\xi = e^{-c} \quad (3)$$

Also,  $P(1)$  is the fraction of area covered by only one fiber,  $P(2)$  is the fraction of area covered by two fibers (so this represents the area of two-fiber crossings), and  $P(3)$  is the fraction of area covered by three fibers (i.e., by a double crossing of fibers).

### Area Covered by Multiple Fibers in Fiber Crossings

In general, a point covered by  $n$  fibers is covered by  $n-1$  crossings. So  $A_c$ , the total area of fiber crossings per unit area, is given by

$$A_c = \sum_{n=2}^{\infty} (n-1)P(n) \quad (4)$$

Eq. (4) can be re-written in terms of the Poisson distribution of Eq. (1)

$$A_c = \sum_{n=2}^{\infty} (n-1) \frac{e^{-c} c^n}{n!} \quad (5)$$

or

$$A_c = e^{-c} \sum_{n=2}^{\infty} (n-1) \frac{c^n}{n!} \quad (6)$$

Expanding Eq. (6)

$$A_c = e^{-c} \left[ \frac{c^2}{2!} + \frac{2c^3}{3!} + \frac{3c^4}{4!} + \dots + \frac{(n-1)c^n}{n!} + \dots \right] \quad (7)$$

Recall that

$$e^c = \sum_{n=1}^{\infty} \frac{c^n}{n!} \quad (8)$$

which, combined with Eq. (6) gives

$$A_c = e^{-c} \left[ 1 + c + \frac{2c^2}{2!} + \frac{3c^3}{3!} + \dots + \frac{nc^n}{n!} + \dots - e^c \right] \quad (9)$$

Simplifying,

$$A_c = e^{-c} \left[ 1 + \left\{ c + c^2 + \frac{c^3}{2!} + \dots + \frac{c^n}{(n-1)!} + \dots \right\} - e^c \right] \quad (10)$$

Since the term in the interior brackets is  $ce^c$ , Eq. (10) can then be written

$$A_c = e^{-c} + c - 1 \quad (11)$$

Introducing Eq. (3), Eq. (11) can be written

$$A_c = \xi + c - 1 \quad (12)$$

which upon rearrangement, becomes

$$A_c = c - (1 - \xi) \quad (13)$$

In this form, it is seen that the total area of fiber crossings per unit area is the difference between the total coverage and the fraction of the unit area covered by fibers.

### **Number of Fiber Crossings**

Fiber crossings form the vertices of the polygon pores in the fabric. The number of crossings is therefore a needed quantity as it is related to the number of polygon pores.

The mean area of a fiber crossing,  $\alpha_c$  is given by

$$\alpha_c = \frac{\pi}{2} w^2 \quad (14)$$

where  $w$  is the projected width of a fiber [3]. For round fibers,  $w$  is the fiber diameter.

The number of fiber crossings per unit area,  $n_c$  can now be obtained from the total crossing area fraction and the mean area of a single crossing

$$n_c = \frac{A_c}{\alpha_c} = \frac{2}{\pi w^2} (e^{-c} + c - 1) \quad (15)$$

For small coverage, the exponential above can be expanded to give

$$n_c \cong \frac{2}{\pi \cdot w^2} \cdot \left( 1 - c + \frac{c^2}{2} - \frac{c^3}{6} + c - 1 \right) \quad (15A)$$

Then

$$n_c \cong \frac{c^2}{\pi \cdot w^2} = \frac{(n_f \cdot \ell)^2}{\pi} \quad (15B)$$

where

$n_f$  is the total number of fibers per unit area  
 $\ell$  is the fiber length

Equation 15B is the Kallmes and Corte [3] result for small  $c$ .

### **Number of Polygon Pores per Unit Area**

Per Kallmes and Corte [3], the number of polygon pores per unit area,  $N_p$ , is given by

$$N_p = (n_c - n_f) e^{-c} \quad (16)$$

Then the mean pore area,  $\langle A_p \rangle$ , is given by the fraction of open area divided by the number of pores per unit area

$$\langle A_p \rangle = \frac{\xi}{N_p} \quad (17)$$

Substituting Eqs. (2), (3), (15), and (16) into Eq. (17), gives

$$\langle A_p \rangle = \frac{\pi w^2}{2} \frac{1}{(e^{-c} + c - 1) - \frac{\pi}{2} \frac{wc}{\ell}} \quad (18)$$

When  $w \ll \ell$ , which is the case for continuous fine fibers, the mean pore area is approximately

$$\langle A_p \rangle \cong \frac{\pi w^2}{2} \frac{1}{e^{-c} + c - 1} \quad (19)$$

Again, for small  $c$ , the denominator of Eq. 19 reduces to  $c^2$ . Then,

$$\langle A_p \rangle = \frac{\pi \cdot w^2}{c^2} = \frac{\pi}{(n_f \cdot \ell)^2} \quad (19A)$$

With this relationship, Kallmes and Corte [3] determined that the pore area is inversely proportional to the square of the total length of fiber deposited.

### Wetted Perimeter

The polygons formed by randomly deposited continuous fibers have numbers of sides ranging from 3 to about 10. Miles [4] showed that the mean number of polygon sides is four. The wetted perimeter of a mean pore is then just four times the average length of a free fiber segment between crossings. Let  $\lambda$  denote the average length of a free fiber segment between fiber crossings. From the total length of fiber and the total number of fiber crossings per unit area  $\lambda$  can be obtained as:

$$\lambda = \frac{n_f \times \ell}{2n_c} \quad (20)$$

The factor of two arises since a single crossing cuts two fibers. Hence to divide the total fiber length by the total number of "cuts", as it were, the number of crossings must be counted twice. Using Eqs. (2) and (15), Eq. (20) can be rewritten:

$$\lambda = \frac{\pi w}{4(e^{-c} + c - 1)} \quad (21)$$

For small  $c$ , Eq. (21) reduces to the Kallmes and Corte [3] equivalent,

$$\lambda = \frac{\pi}{2} \cdot \frac{1}{n_f \cdot \ell} \quad \text{Equation A27}$$

This result for a very small coverage of fibers again points out that the dimensions in the stochastic structure depend upon the total length of fibers deposited. In this case the mean distance between fiber intersections, or the mean free fiber length, is inversely proportional to the total length of fiber deposited per unit area.\*

\* It is a counterintuitive characteristic of the random geometry that the mean segment length and the segment length distribution for a randomly cut line do not depend upon the width of the cut. Hence the mean length of a free fiber segment between fiber crossings does not depend upon the fiber width. What does change with the width of fibers is the number of free fiber segments, i.e., the total length of free segments decreases as fiber width increases.

### Hydraulic Radius and Mean Pore Diameter

The hydraulic radius,  $R_h$  is defined as the pore area divided by the wetted perimeter of the pore. From the development above,

$$R_h = \frac{\langle A_p \rangle}{4\lambda} \quad (22)$$

Substituting Eqs. (19) and (21) into Eq. (22) gives:

$$R_h = \frac{w}{2c} \quad (23)$$

By analogy to a cylindrical pore, the mean pore diameter,  $D_{p,mean}$ , is four times the hydraulic radius. So,

$$D_{p,mean} = \frac{2w}{c} = \frac{2}{n_f \ell} \quad (24)$$

As noted above, the one assumption incorporated in this result is that  $w \ll \ell$

### Maximum Pore Diameter

Per Lombard, Rollin, and Wolff [5], Matheron [6] characterized pore sizes in random fiber sheets in terms of the largest circles which can be inscribed in the polygon pores of the two dimensional structure. The resulting pore size distribution density function is given as

$$f(\sigma) = 2(\sigma^2 r^2 + \sigma) e^{-2\sigma} \quad (25)$$

Where  $r$  is the radius of the idealized pore and  $\sigma$  is the total length of fiber per unit area. The cumulative pore size distribution,  $F(\sigma)$ , the fraction of pores smaller than size  $r$ , is given by

$$F(\sigma) = 1 - (1 + \sigma)^2 e^{-2\sigma} \quad (26)$$

These two functions are plotted in *Figure 1*, below, where  $x = \sigma r$

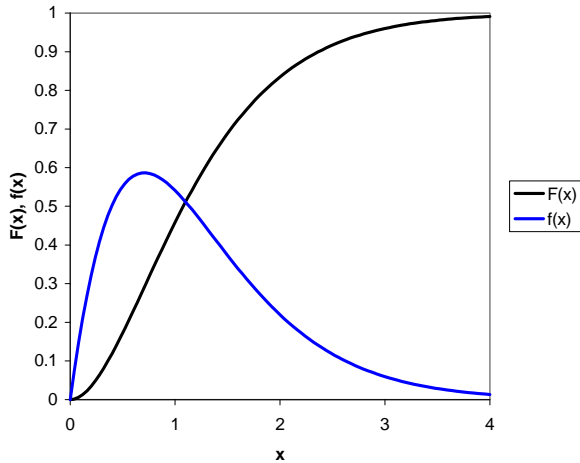


FIGURE 1. Cumulative distribution function  $F(x)$  and distribution density function  $f(x)$  for pore size.

For this distribution, the mean radius,  $r_m = 1.25 / \sigma$  and  $F(x) \cong 0.99$  when  $r = 3.8 / \sigma$ . That is, 99% of the pores are smaller than about  $r = 3.8 / \sigma$ . If  $r = 3.8 / \sigma$  is taken to approximate the size of the largest pore, then

$$D_{p,max} \cong 3D_{p,mean} \quad (27)$$

Combining this with Eq. (24) gives

$$D_{p,max} \cong \frac{6w}{c} \quad (28)$$

From the analysis so far, pore size is proportional to fiber width and inversely proportional to the coverage of fibers in the fabric layer. Recalling the definition of fiber coverage in Eq. (2) above, we have the result

$$D_{p,max} \cong \frac{6}{n_f \ell} \quad (29)$$

Again, the key dimensions of the stochastic structure are determined solely by the total length of fiber randomly deposited to form the nonwoven fabric.

### **The Three Dimensional Fabric and the Problem of Self Similarity**

The analysis so far assumes that all fibers are randomly deposited in a single plane. This is the reason that the results show pore size monotonically decreasing as more fibers are deposited. From

intuition and experience one recognizes that this must be the case as the first few fibers are deposited. But as more and more fibers are deposited, the real fabric becomes three dimensional. In fact, as a thick layer of fibers is built up, and assuming the void fraction of the layer stays constant, the pore geometry can be presumed to be independent of the number of fibers deposited. Deep within a thick layer of fibers, a fluid penetrating perpendicular to the plane of fiber deposition will “see” the same pore structure no matter the depth of penetration. The issue, then, is how to view the statistical analysis presented so far, and how to relate it to the three-dimensional fabric structure.

### **Elemental Fiber Deposition Plane**

As mentioned above, the earlier statistical analyses of the stochastic structure of paper were valid for only very small fiber coverages of the deposition plane. Typically then, these analyses are interpreted as applying to an “elemental plane” of the fabric. The elemental planes are considered to be stacked to form the full fabric. The same approach is used here. Following the outline of Lombard, Rollin, and Wolff [5], the elemental fiber deposition plane is taken to be a fabric plane with a thickness of two fibers. *Figure 2* below, patterned after *Figure 4* in [5], illustrates the elemental plane.

Within the framework of the present analysis, the elemental plane, then, includes all fibers with centers on or within the plane boundaries. This means, in principle that as many as three fibers can intersect within the elemental plane. Hence, the analysis should hold whenever  $P(4) \ll 1$ , where  $P(4)$  is defined by Eq. (1). Note that, as illustrated in the above figure, the analysis is not dependent upon the fibers being round.

### **Interaction between Elemental Planes**

With the elemental fiber deposition plane defined, the next issue is to determine how the overlaying of successive planes affects fabric pore size. The sequence of *Figures 3, 4, and 5* below illustrate the overlaying of three elemental planes.

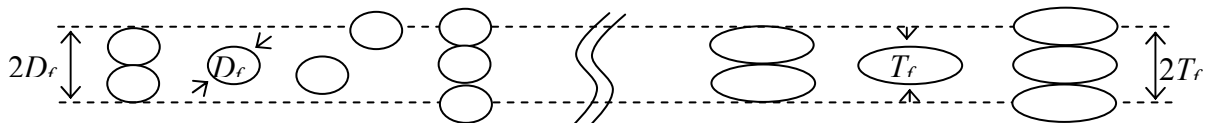


FIGURE 2. Elemental plane illustration

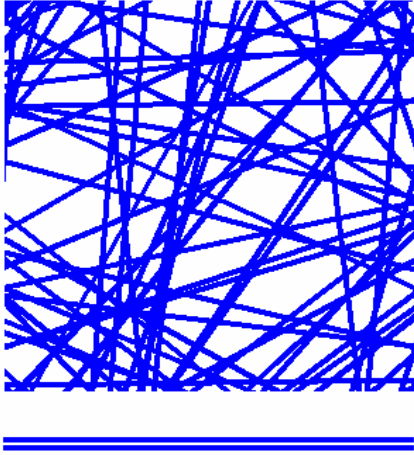


FIGURE 3. A single elemental layer of a random fiber fabric.

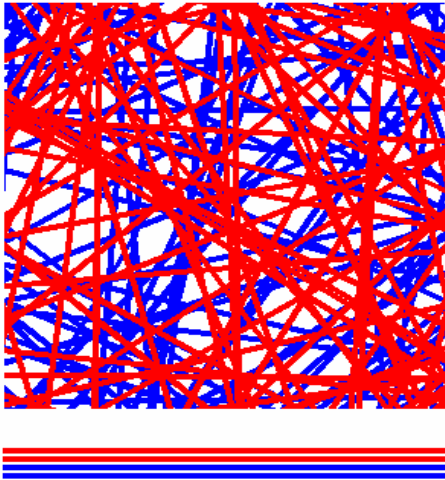


FIGURE 4. Two elemental random fabric layers overlaid.

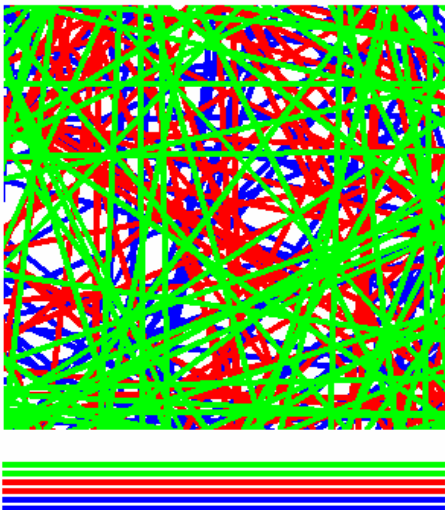


FIGURE 5. Three elemental random fabric layers overlaid.

It is apparent that the total fiber coverage of the deposition area is a linear function of the number of planes overlaid. The relationship between total fiber coverage and pore size is rationalized as follows: From the perspective of the meniscus of a non-wetting fluid approaching the green or topmost plane, it is clear that the pore size encountered is always affected by fibers in the next plane in the fluid path, in this case by the middle or red plane. So, at least two elemental planes always interact to determine the effective pore size in a given plane. It is not clear from the illustration whether the second plane below the top, i.e., the third or blue plane, must be considered as a determinant of the pore size of the first or green plane. Intuition holds that elemental planes far removed from the position of the fluid meniscus do not need to be considered. How many elemental planes must be considered to determine the effective pore size in a given plane can be understood to be dependent upon how densely elemental planes are packed together. This, in turn, depends upon the fiber modulus and whether the sheet is calendered. Straight, stiff, round fibers such as glass fibers will pack with a void fraction exceeding 0.90, while soft deformable fibers can pack to a void fraction below 0.60. So, the number of elemental planes which need to be considered in the determination of fabric pore size is somewhat specific to the materials and method of formation of the fabric. A number of studies in the literature of paper have dealt with the factors affecting the interactions between elemental fiber deposition layers and the density of a sheet [7], [8], [9], [10].

The analysis through Eq. (29) is now construed to describe the elemental layer of a three dimensional nonwoven fabric. Letting  $n_p$  denote the number of elemental planes that must be taken into account together to describe the three dimensional pore structure, the mean pore size can now be written

$$D_{p,mean} = \frac{2}{n_p n_f \ell} \quad (30)$$

For the elementary plane, the total fiber length can be obtained as follows:

$$n_f \ell = \frac{\text{FiberLength}}{\text{UnitArea}} = \frac{\text{LayerThickness SolidsFraction}}{\text{FiberVolume/ UnitLength}} \quad (31)$$

For round fibers,

$$n_f \ell = \frac{2D_f \phi}{\pi D_f^2 / 4} = \frac{8\phi}{\pi D_f} \quad (32)$$

Note that the solids fraction  $\phi$  is 1 minus the void fraction,  $\varepsilon$ . So Eq. (30) can now be written:

$$D_{p,mean} = \frac{\pi D_f}{4n_p(1-\varepsilon)}; n_p \geq 2 \quad (33)$$

In the limit of high void fraction, e.g., for straight stiff fibers, layer-to-layer interactions will be minimal and  $n_p = 2$ . Then,

$$D_{p,mean} = \frac{\pi D_f}{8(1-\varepsilon)} \quad (34)$$

Again, per Eq. 27, the maximum pore size is approximately three times the mean. De Bruyne [11] presented an empirical correlation of the maximum pore size in fibrous media with the same functional form as Eq. 34, but with a numerical coefficient of 1.0. In comparison, the coefficient for this work is  $3\pi/8 = 1.18$ . This represents very good agreement considering that effects of the pore network can easily reduce the apparent pore size and narrow the measured pore size distribution in the liquid intrusion measurements used to measure pore sizes [12].

Eq. (34) is the central result of this section. It represents as a benchmark, the mean of the expected pore size range in a nonwoven fabric.

#### SUMMARY OF LIFSHUTZ MODEL

Lifshutz [1] found a statistical correlation between mean flow pore diameter as measured using an automated Capillary Flow Porometer instrument by Porous Materials Incorporated (PMI), total fiber length per unit area, and fiber diameter for microfiber and nanofiber webs. Lifshutz concludes from this study that a simple stochastic model of the web leads to an exponential distribution of the hydraulic diameter of the pores resulting from the intersection of all the fibers. He also concludes that the mean flow pore diameter can then be shown to be a simple multiple of the mean hydraulic diameter.

In the Lifshutz model, the conversion constant between mean flow pore diameter,  $D_{mf}$ , and mean hydraulic diameter,  $D_h$ , depends on whether one assumes that the pores in a real nonwoven take the form of an orifice or a capillary. If one assumes the orifice model then

$$D_{mf} = 1.337D_h \quad (35)$$

However, if one assumes the capillary model, then

$$D_{mf} = 2.336D_h \quad (36)$$

Lifshutz conducted an extensive set of experiments using wetlaid glass microfiber handsheets and electrospun polymeric nanofiber webs. The range of fiber diameters in these sheets was  $0.3 \mu\text{m}$  to  $6.6 \mu\text{m}$ . The measured mean flow pore diameters ranged from  $1.3 \mu\text{m}$  to  $52.8 \mu\text{m}$ . Note that these sheets were very open structures with basis weights from  $0.28 \text{ g/m}^2$  to  $126 \text{ g/m}^2$  which, for the materials used, translates to a 97-98% porosity or void volume. The statistical correlation made by Lifshutz between modeled results and actual experimental data on real nonwoven webs indicated that the effective length of fiber determining the mean flow pore size is one to two orders of magnitude smaller than the total length of fiber in the web. According to Lifshutz, this suggests that the mean flow pore diameter is determined by a "very thin downstream layer of the web" and appears to depend only on the diameter of the fiber and the basis length of the web. Lifshutz defines basis length as the total length of fiber per unit area of the mat:

$$\Lambda = \frac{4G}{\pi D_f^2 \rho} \quad (37)$$

where  $G$  is the mass per unit area of the fiber mat,  $D_f$  is the fiber diameter, and  $\rho$  is fiber material density.

The correlations by Lifshutz found that the results were not a large function of the model chosen. Rather, one could do a direct correlation between the mean flow pore diameter, the fiber diameter and the basis length. The relationship being:

$$D_{mf} = 32.28D_f^{0.2354}\Lambda^{-0.5260} \quad (38)$$

For the data examined by Lifshutz,  $R^2 = 0.98$ , which indicates an acceptable fit.

#### PART 2 – USE OF MODELS TO DESIGN FABRICS TO MEET PORE SPECIFICATIONS

New nonwovens applications in areas such as filtration require a media designed to particular pore size specifications in the 3 to 20 micron range. Our objective was to create two fabrics with mean flow pore diameters of 2 and 5 microns respectively. We applied the two models described in Part 1 to aid in fabric design. The comparison of our experimental results to the theoretical results is presented here.

#### EXPERIMENTAL RESULTS

To test these two models, we selected target ranges for two fabrics:

Fabric 1

Mean Pore Diameter = 5 $\mu$ m  
Porosity = 70%

Fabric 2

Mean Pore Diameter = 2 $\mu$ m  
Porosity = 80%

At the fabric design stage, it was unknown if the Lifshutz model [1] or the Bryner model (see Part 1 of this paper) would provide more accurate results. Therefore, a comparison of predicted mean flow pore diameters was done using the two models. Fabric specifications (fabric basis weights, fiber diameters, fabric thicknesses) for the experimental work were

chosen to hopefully bracket the desired range of 5-10 microns for fabric 1 (samples A through E) and 2-3 microns for fabric 2 (sample H). For Fabrics A and H a thickness specification was given and the required basis weight was calculated using the model. For Fabrics B through E, the basis weights were specified and the thickness was calculated using the model. *Table I.* shows the calculated parameters using the Bryner model. Note that the void volume (porosity)  $\varepsilon$  is

$$\varepsilon = 1 - \phi \quad (39)$$

TABLE I. Bryner model calculations

	A	B	C	D	E	H
<b>Inputs</b>						
$D_{p,mean}$ ( $\mu$ m)	5	5	5	5	5	2
$\phi$	0.3	0.3	0.3	0.3	0.3	0.2
$\rho$ (g/cm <sup>3</sup> )	1.14	1.14	1.14	1.14	1.14	1.14
$T$ (mm)	0.1	-	-	-	-	0.5
$G$ (g/m <sup>2</sup> )	-	50	65	96	111	-
<b>Outputs</b>						
$T$ (mm)	-	0.15	0.19	0.28	0.32	-
$G$ (g/m <sup>2</sup> )	34	-	-	-	-	114
$D_f$ ( $\mu$ m)	3.82	3.82	3.82	3.82	3.82	1.02

The resultant fiber diameter of the Bryner model was then used as input to the Lifshutz model. Results of predicted pore sizes are shown in *Table II.* Note that the mean flow pore diameters  $D_{mf}$  predicted by Lifshutz are considerably larger than those predicted by Bryner. The average hydraulic diameter,  $D_{h,avg}$ , shown in the table is the average of the hydraulic diameter determined from the orifice and capillary models, Eqs. (35) and (36), respectively. The fabric thickness,  $T$ , or alternately, the basis weight  $G$ , may be found using (accounting for the units used in *Table II.*)

$$T = \frac{G}{1000 \cdot \rho \phi} \quad (40)$$

The details of the fabric specifications are shown in *Table III.* The desired basis weight (taken from *Table II.*) is used as an input, as are the material density of

the island and sea polymers,  $\rho_i$  and  $\rho_s$ , respectively, as well as the number of islands,  $n_i$ , and the weight fraction island polymer,  $w_i$ . The total area of the island in the sea fiber is found using (and accounting for the units used in *Table III.*)

$$A_f = \frac{dpf \cdot 10^5}{9[\rho_i w_i + \rho_s (1 - w_i)]} \quad (41)$$

The fabric basis weight before melting out the sea polymer,  $G_{bm}$ , can be calculated from

$$G_{bm} = G + G(1 - w_i) \frac{\rho_s}{\rho_i} \quad (42)$$

TABLE II. Lifshutz model calculations

	A	B	C	D	E	H
<b>Inputs</b>						
$D_f$ ( $\mu\text{m}$ )	3.82	3.82	3.82	3.82	3.82	1.02
$\phi$	0.3	0.3	0.3	0.3	0.3	0.2
$\rho$ ( $\text{g}/\text{cm}^3$ )	1.14	1.14	1.14	1.14	1.14	1.14
$T$ (mm)	0.1	-	-	-	-	0.5
$G$ ( $\text{g}/\text{m}^2$ )	-	50	65	96	111	-
<b>Outputs</b>						
$T$ (mm)	-	0.15	0.19	0.28	0.32	-
$G$ ( $\text{g}/\text{m}^2$ )	34	-	-	-	-	114
$\Lambda$ (1/m)	2.6	3.8	5	7.3	8.5	122.7
$D_{mf}$ ( $\mu\text{m}$ )	26.7	21.8	19	15.5	14.4	2.6
$D_{h,orifice}$ ( $\mu\text{m}$ )	19.9	16.3	14.2	11.6	10.7	1.9
$D_{h,capillary}$ ( $\mu\text{m}$ )	11.4	9.3	8.1	6.6	6.1	1.1
$D_{h,avg}$ ( $\mu\text{m}$ )	15.7	12.8	11.2	9.1	8.4	1.5

TABLE III. Calculation of INS fiber diameter, number of islands, and basis weight

	A	B	C	D	E	H
<b>Inputs</b>						
$G$ ( $\text{g}/\text{m}^2$ )	34	50	65	96	111	114
dpf	3	3	3	3	3	1
$\rho_i$ ( $\text{g}/\text{cm}^3$ )	1.14	1.14	1.14	1.14	1.14	1.14
$\rho_s$ ( $\text{g}/\text{cm}^3$ )	1.36	1.36	1.36	1.36	1.36	1.36
$n_i$	18	18	18	18	18	72
$w_i$	0.75	0.75	0.75	0.75	0.75	0.65
<b>Outputs</b>						
$A_f$ ( $\mu\text{m}^2$ )	279	279	279	279	279	91
$D_i$ ( $\mu\text{m}$ )	3.85	3.85	3.85	3.85	3.85	1.02
$G_{bm}$ ( $\text{g}/\text{m}^2$ )	44	65	84	125	144	162

Note that although a fabric thickness is required for the Lifshutz model (in order to determine the basis weight, if not independently specified), the facilities we used had no means to control fabric thickness. The web laydown density was controlled to provide a specified basis weight and fiber diameter only. The web could be calendered using a set of fixed rolls with either smooth or patterned surfaces. A gap between the rolls could not be adjusted and the weight or pressure of the rolls was not adjustable.

The only adjustment was roll temperature. In our case, we used smooth rolls at ambient temperature so as to minimize disruptions to the random web while providing some degree of strength for handling purposes only. Even if we had been able to control fabric thickness at this stage of manufacturing, the post processing required to remove the sea polymer would likely have changed the thickness anyway. This lack of thickness control proved to be a critical factor in our inability to directly apply the Bryner

model to fabric design. This point is explored in further detail later.

In order to manufacture the correct fiber diameters, our experience indicated that Zytel 101 nylon and Eastman AQ55 polyester could be co-spun as islands-in-the-sea fibers. Using this polyester for the sea polymer, it could later be dissolved in water to leave the small nylon microfibers of the desired diameters. Selection of weight fractions of the two polymers and as-spun fiber diameters were done within the specification limits of the spunbond equipment at North Carolina State University nonwovens laboratory. These fiber webs were not bonded in any way during manufacturing. It was assumed that mechanical strength required in use could be achieved at a subsequent processing step.

This posed a problem during the dissolving of the polyester polymer. Because there was little mechanical strength in the webs, they could not be placed in turbulent flows such as a jet dyer or washing machine. Thus, small samples were supported on a screen and a hot caustic solution soak followed by a hot water rinse was used to dissolve the polyester for PMI testing. SEM photographs of two samples (*Figures 6-9*) illustrate the difficulty in separating the island and sea polymers. The photographs also clearly show the tendency of the island fibers to remain bundled rather than distribute independently. Despite this tendency, the measured mean flow pore diameters still indicate a close fit to the predictive models.

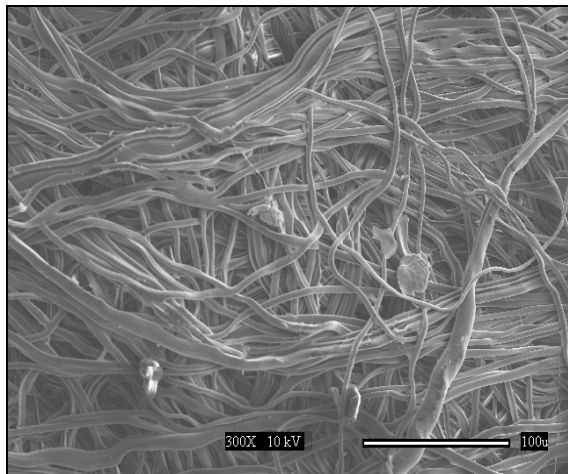


FIGURE 6. SEM of Fabric Sample D Surface

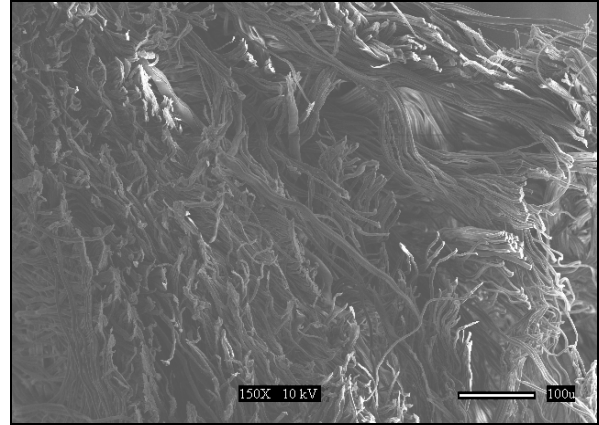


FIGURE 7. SEM of Fabric Sample D Cross Section

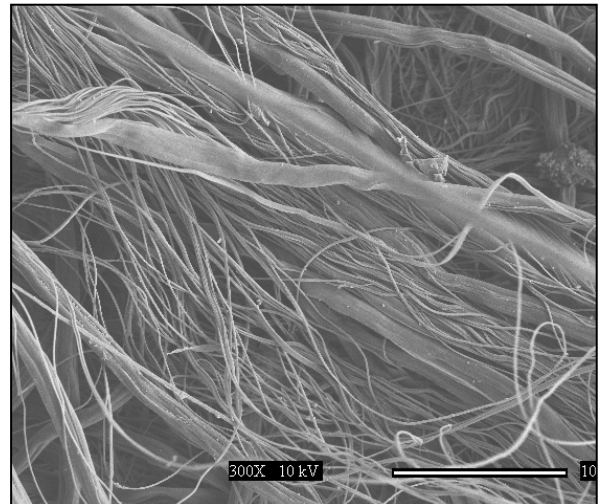


FIGURE 8. SEM of Fabric Sample H Surface

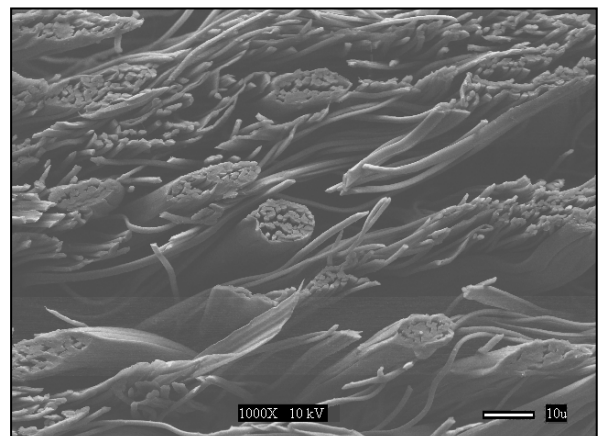


FIGURE 9. SEM of Fabric Sample H Cross Section

Our tests resulted in fabrics that were thicker than our specifications. As a result, the fabrics were much more porous. For comparison to the models, the actual measurements of fabric thickness, basis weight and porosity were used to recalculate the predicted values. The measured values and recalculated predictions are shown in *Table IV*.

Using the actual fiber fraction to recalculate the predicted mean flow pore diameters  $D_{mf}$  in the Bryner model, there is excellent correlation between the predicted and the measured mean flow pore diameters using PMI porometry instruments. This comparison is shown in *Figure 10*. The regression line used was forced to a zero intercept to provide a simple conversion between manufacturing specifications and pore sizes. In this case, to achieve accurate results, manufacturing specifications would have to include fiber size, fabric thickness and porosity (or fiber volume fraction). As previously

mentioned, these parameters are not typically those that are set during fabric specification.

*Figure 11* shows the correlation between the PMI data and the results predicted by Lifshutz. Although a linear curve fit is good, the Lifshutz model results in a predicted mean flow pore that is roughly twice the measured mean flow pore diameter.

An interesting phenomenon is shown in *Figure 12*. If one averages the predicted hydraulic diameters using the capillary and orifice models within Lifshutz, the predicted hydraulic diameter is roughly equal to the measured mean flow pore diameter. We found that this parameter can serve as a better predictor during fabric design for the measured mean flow pore diameter than the value derived by Lifshutz. Note that the greatest divergence occurs at small pore sizes. Using this approach, one could design a fabric using manufacturing specifications of fiber size and basis weight, while excluding fabric thickness, which are much more common specification terms.

TABLE IV. Measured values and recalculated predictions

	A	B	C	D	E	H
Measured						
$T$ (mm)	0.314	0.343	0.336	0.469	0.506	0.801
PMI $D_{mf}$ ( $\mu\text{m}$ )	15.7	11.7	10	8.8	8.4	3.5
$G$ ( $\text{g}/\text{m}^2$ )	34.2	50	65	96	111	100
Recalculated						
$\epsilon$	0.9	0.87	0.83	0.82	0.81	0.89
$\Lambda$ (1/m)	2.6	3.8	4.9	7.2	8.4	106.4
$D_{p,mean}$ ( $\mu\text{m}$ )	15.9	11.9	9	8.5	7.9	3.7
$D_{mf}$ ( $\mu\text{m}$ )	26.9	22	19.2	15.6	14.5	2.8
$D_{h,avg}$ ( $\mu\text{m}$ )	15.8	13	11.3	9.2	8.5	1.6

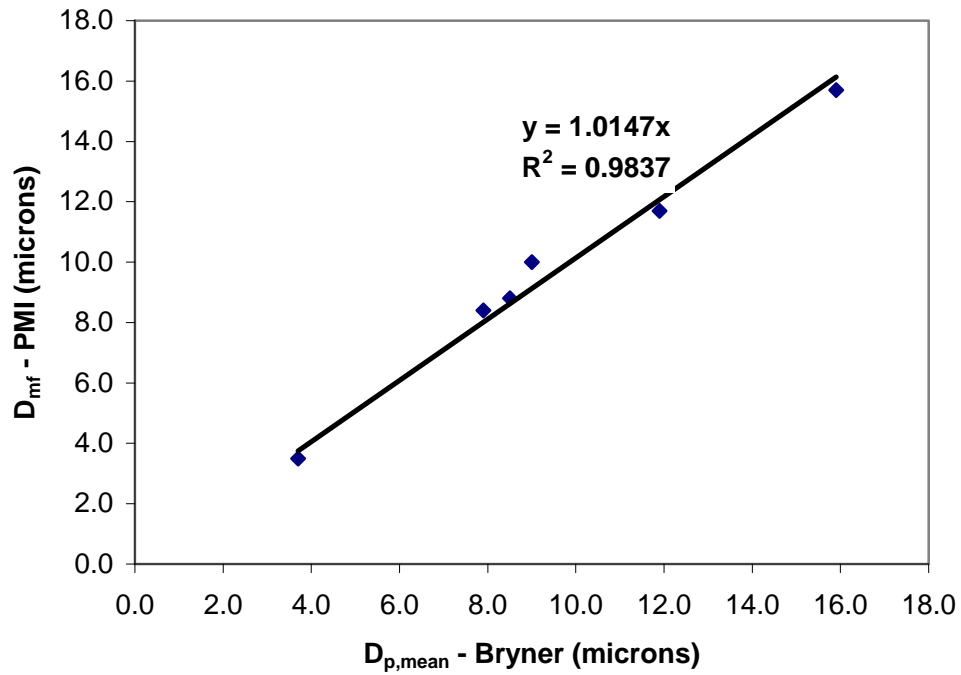


FIGURE 10. PMI data versus Bryner model for mean pore diameter

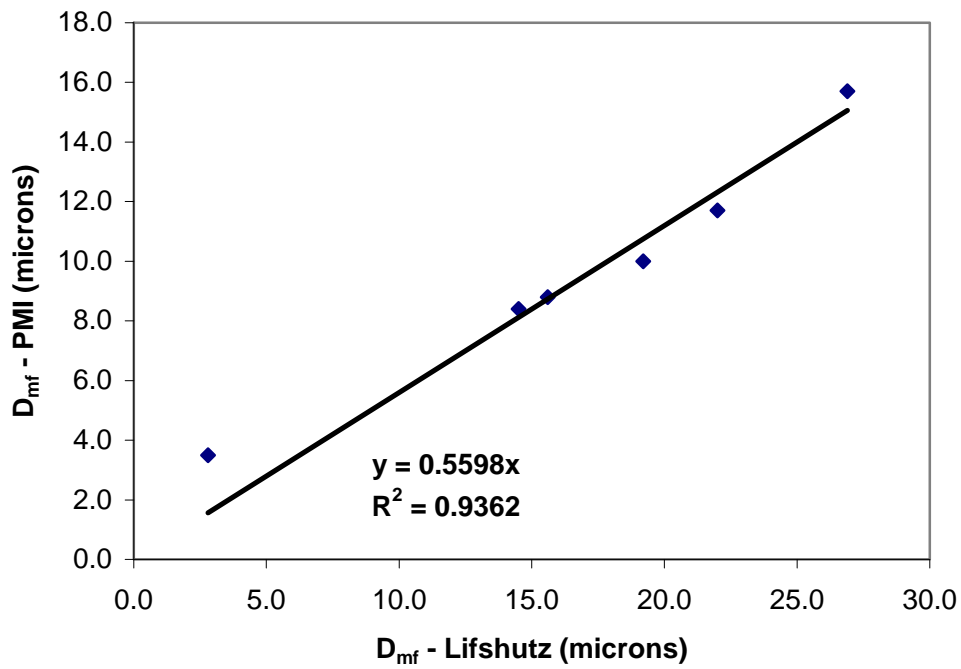


FIGURE 11. PMI data versus Lifshutz model for mean flow pore diameter

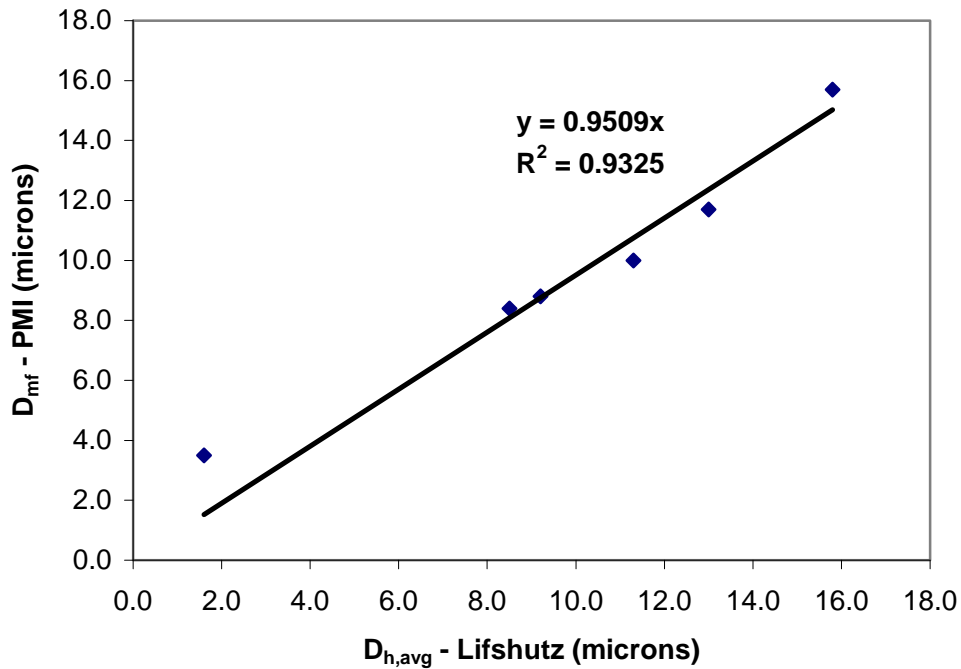


FIGURE 12. PMI versus calculated average hydraulic diameter using Lifshutz

### SUMMARY AND CONCLUSIONS

In this paper, an alternative to the Lifshutz approach to modeling pore size has been developed. The Bryner model relates fiber size and fiber volume fraction to average and maximum pore size in a nonwoven sheet. It is based on the notion that fiber deposition during the fabric formation process is a Poisson process. The approach is first to determine the open pore area. Then the total number of pores is determined. From these two, the mean pore area is established. Pores in nonwoven fabrics are polygons with sides formed by the free length of fibers between crossings. The characteristics of the general nature of the polygons are known, so the number and length of sides is used to determine the average wetted perimeter of a pore. The average perimeter and the pore area are used to determine the pore hydraulic radius from which the mean pore size obtained. The stochastic structure results in a pore size distribution for which the maximum size is known in terms of the mean pore size. Bryner's modeling results for nonwoven fabrics show that the mean pore size,  $D_{p,mean}$ , is directly proportional to fiber size and inversely proportional to the fiber volume fraction,  $\phi$ . It also shows that the maximum pore diameter is roughly three times the size of the mean pore diameter.

We found that the primary difference in the two models is the influence of fabric porosity (or alternatively, fabric thickness at a given basis weight) on mean pore diameter. This is most likely related to the relative stiffness of the fibers and the relative openness of the structures used for development of the models. Lifshutz used stiff glass fibers in very open webs (>97% porosity) to verify his conclusions. Our more dense fabrics (80-90% porosity) and Bryner's model allows for the use of less rigid fibers that can have more of a tendency to pack. This is true even though we assumed only a two layer interaction which Bryner ascribes primarily to straight, stiff fibers.

An exercise to calender these fabrics to various thicknesses and then measure the pore diameters would be interesting to see how these models track measured results as porosity is further decreased. Lifshutz predicts that the mean flow pore diameter is independent of porosity (and therefore thickness) as long as the overall fabric remains highly porous; so there should be no change in the pore size as a result of some light calendering. Bryner, on the other hand, would predict a linear relationship, with the pore diameters decreasing as the thickness (and porosity) decreases. The accuracy of the Bryner model when corrected for fabric thickness leads one to believe that this is the more complete model and would be applicable over a broader range of fabric porosity and

fiber types. If specific manufacturing equipment capabilities are such that thickness can be controlled, the Bryner model is definitely preferred. Although not as accurate as the Bryner model, the Lifshutz approach is likely a more practical one in cases where fabric thickness cannot be independently controlled, and appears to be fairly good in terms of providing a fabric of the desired pore diameters.

The removal of the sea polymer can be a demanding task. Polymer selection, web bonding, as-spun fabric handling, sea polymer removal, separation of the island fiber groups and final fabric calendering and finishing are all fertile areas for future optimization. The materials and methods chosen for each of these can have significant impact on the fabric thickness (and porosity) when compared to the as-spun condition. Use of either of these models at the fabric design stage provide a good starting point for fabric development aimed at meeting specified mean flow pore diameters.

### Conclusions

1. We found that for fabrics with porosities in the range of 80% to 90%, made from flexible fibers, Lifshutz' average hydraulic pore diameter is a better predictor of the measured mean flow pore diameter than the value he calculates for this parameter.
2. The mean pore diameter as calculated by Bryner is an excellent predictor of the measured mean flow pore diameter.
3. Use of the Bryner model to design fabrics to pore size specifications requires the ability to control fabric porosity (thickness) for a given basis weight and fiber diameter. The Lifshutz model can be applied (using average hydraulic diameter to predict mean flow pore diameter) fairly accurately with only basis weight and fiber diameter being controlled. Note that Lifshutz tends to deviate as fibers and pore sizes become smaller. Although it was beyond the scope of our experimental work, we suspect that the Lifshutz model will also become less accurate as the fabric porosity continues to decrease (below 80%) and packing or layering become more pronounced.
4. Spunbonded bicomponent fibers in the form of islands-in-the-sea fibers provide excellent fiber diameter control and can be used to precisely design fabrics to meet pore size specifications in the 3 to 20 micron range.

### **ACKNOWLEDGEMENTS**

The authors wish to thank Dr. Behnam Pourdeyhimi, Sherwood Wallace and Stephen Sharp of the Nonwovens Cooperative Research Center at North Carolina State University for their help and efforts in making these sample fabrics.

### **REFERENCES**

- [1] Lifshutz, N., On the "Mean Flow" Pore Size Distribution of Microfiber and Nanofiber Webs, *International Nonwovens Journal*, 14 (1), 18-24 (2005).
- [2] Deng, M. and Dodson, C.J.T., Paper: An Engineered Stochastic Structure, TAPPI Press, Atlanta, GA, 1994.
- [3] Kallmes, O. and Corte, H., The Structure of Paper in the Statistical Geometry of an Ideal Two Dimensional Fiber Network TAPPI Journal, 43 (9), 737-752 (1960).
- [4] Miles, R.E., Random Polygons Determined by Lines in a Plane, *Proc. Nat. Acad. Sci. USA*, 901-907 and 1157-1160 (1964).
- [5] Lombard, G., Rollin, A., and Wolff, C., Theoretical and Experimental Opening Sizes of Heat-bonded Geotextiles, *Textile Research Journal*, 208 (1989).
- [6] Matheron, Ensembles Fermes Aleatoires, Ensembles Semi-Markovians et Polyedres Poissoniens, *Adv. Appl. Prop.*, 4, 508-541 (1972).
- [7] Amiri, R., et al, The Apparent Density of Paper, *Journal of Pulp and Paper Science*, 20 (5), j142 (1994).
- [8] Steadman, R. and Luner, P., The Effect of Wet Fiber Flexibility of Sheet Apparent Density, *Papermaking Raw Materials*, V. Punton, ed. Vol. 1, 311-338 (1985).
- [9] Kallmes, O., Corte, H., and Bernier, G., The Structure of Paper II. The Statistical Geometry of a Multiplanar Fiber Network, *TAPPI Journal*, 44 (7), 519 (1961).
- [10] Gorres, J., Sinclair, C.S., and Tallentire, A., An Interactive Multi-planar Model of Paper Structure, *Paper and Timber* 1/1989, 54 (1989).

- [11] De Bruyne, R, Properties of Metal Fiber Filter Media. In Recent Developments in Filter Media and Their Applications: Proceedings of the International Symposium, Brussels, September 18-19, 1980; Eds, Weiler, R and De Bruyne, R; Koninklijke Vlaamse Ingenieursvereniging: Antwerp, 1980; pages 2.1.1 – 2.5.8.
- [12] Bryner, M. A., A Unified Statistical Analysis of Two-Phase Flows Through Porous Media, Dissertation: Clarkson University, 1973

#### **AUTHORS' ADDRESSES**

**Glen D. Simmonds, John D. Bomberger**

DuPont  
Central Research & Development  
Experimental Station  
P.O. Box 80304  
Wilmington, DE 19880-0304  
USA

**Michael Bryner**

E.I. Du Pont de Nemours & Co.,  
5401 Jefferson Davis Highway  
Richmond, Virginia 23234  
USA